Bubble nonlinear dynamics and stimulated scattering process*

Jie Shi(时洁)[1,2], De-Sen Yang(杨德森)[1,2], Sheng-Guo Shi(时胜国)[1,2], Bo Hu(胡博)[1,2,†], Hao-Yang Zhang(张昊阳)[1,2], and Shi-Yong Hu(胡诗涌)[1]

[1] *College of Underwater Acoustic Engineering, Harbin Engineering University, Harbin* 150001, *China*
[2] *Acoustic Science and Technology Laboratory, Harbin Engineering University, Harbin* 150001, *China*

(Received 12 July 2015; revised manuscript received 25 August 2015; published online 20 December 2015)

A complete understanding of the bubble dynamics is deemed necessary in order to achieve their full potential applications in industry and medicine. For this purpose it is first needed to expand our knowledge of a single bubble behavior under different possible conditions including the frequency and pressure variations of the sound field. In addition, stimulated scattering of sound on a bubble is a special effect in sound field, and its characteristics are associated with bubble oscillation mode. A bubble in liquid can be considered as a representative example of nonlinear dynamical system theory with its resonance, and its dynamics characteristics can be described by the Keller–Miksis equation. The nonlinear dynamics of an acoustically excited gas bubble in water is investigated by using theoretical and numerical analysis methods. Our results show its strongly nonlinear behavior with respect to the pressure amplitude and excitation frequency as the control parameters, and give an intuitive insight into stimulated sound scattering on a bubble. It is seen that the stimulated sound scattering is different from common dynamical behaviors, such as bifurcation and chaos, which is the result of the nonlinear resonance of a bubble under the excitation of a high amplitude acoustic sound wave essentially. The numerical analysis results show that the threshold of stimulated sound scattering is smaller than those of bifurcation and chaos in the common condition.

Keywords: bubble dynamics, nonlinear resonance, anti-Stokes and Stokes component

PACS: 43.25.Rq, 43.25.Ts, 43.25.Yw **DOI:** 10.1088/1674-1056/25/2/024304

1. Introduction

A single gas bubble can be driven to oscillate in a liquid medium when it is exposed to a high-amplitude, high-frequency acoustic wave. In the past, several bubble models were established by Rayleigh and Plesset, Noltingk and Neppiras, Keller and Miksis[1] one after another, and various methods were also developed to analyze these models. The knowledge of bubbles and their behaviors is continually discussed.[2–4] It is seen that bubbles and cavitation are closely connected and often both are discussed together. Most papers on cavitation contain insight into bubbles and their dynamics,[5,6] and point out bubble oscillations result in the radiation of acoustic waves.

In recent years, the knowledge of the complex nonlinear dynamics characteristics of bubble oscillation driven by acoustic waves was continually argued. Yang *et al.* further enriched the theoretical and experimental results of the single cavitation bubble oscillation. The influences of acoustic pressure, frequency, initial bubble radius, surface tension, viscosity and other control parameters on the dynamics of a single acoustically driven bubble were studied in detail.[7] Zhu *et al*. discovered that the pulsing bubble, as a nonlinear oscillator, could be treated as a secondary radiation source, and the acoustic field showed the characteristics of strong nonlinearity and attenuation.[8] In fact, the second harmonic and higher ones with arbitrary acoustic pressure amplitudes can be generated naturally, however, the sub-harmonics can only appear when the acoustic pressure amplitude reaches or exceeds a certain suitable threshold.[9] The generation mechanism of bubble sub-harmonic oscillation was illustrated in many previous research results, and the acoustic chaos phenomenon caused by the nonlinear bubble oscillations was studied.[10,11] Cheng *et al*. studied the bubble dynamics in ultrasonic sonoporation by constructing a model of cavitated bubbles and changing the parameters, such as the ultrasonic signal frequency, acoustic pressure, initial radius of bubbles and viscosity of the fluid.[12] Considering liquid compressibility and regarding water as a work medium, the effects of acoustic frequency, acoustic pressure, initial radius of bubble, liquid surface tension, and viscosity coefficient on bubble motion state were studied, and further analysis of the relationship between cavitation treatment effect and bubble motion state showed that the motion bubbles in the chaotic state could improve the acoustic cavitation degradation ability of organic pollutants.[13,14] Lauterborn *et al*. further enriched the theoretical and experimental results of the single cavitation bubble oscillation.[15] The influences of acoustic pressure, frequency, initial bubble radius, surface tension, viscosity and other control parameters on the dynamics of a single acoustically driven bubble were studied

*Project supported by the Program for Changjiang Scholars and Innovative Research Team in University, China (Grant No. IRT1228) and the Young Scientists Fund of the National Natural Science Foundation of China (Grant Nos. 11204050 and 11204049).

†Corresponding author. E-mail: kidd1105@sina.com

© 2016 Chinese Physical Society and IOP Publishing Ltd

in detail.[16,17]

In addition, the stimulated sound scattering is a particular effect, and its character is associated with the special oscillation mode (for example, the bubble oscillation mode in liquids) in the interaction. When a bubble is driven periodically by an acoustic wave, it responds to the driving with nonlinear oscillations,[18,19] then it can be regarded as a generated sound source. Such processes as sound scattering and even stimulated sound scattering are possibly associated with it. Zabolotskaya[20] and Butkovskii *et al.*[21] were the first ones to do research on stimulated combination sound scattering in a liquid with gas bubbles, and this effect could be analogous to stimulated combination light scattering, and the natural frequency of bubbles would shift, with the cubic nonlinearity of bubble oscillations considered. During the experiment of this effect, the amplification of Stokes component was also observed. However, the work by Zabolotskaya *et al.* was only in the framework of wave process theory, and the oscillation characteristics of the bubble were not fully taken into consideration. A further important question is what the relationship between the bubble oscillations and stimulated sound scattering process is.

The purpose of this paper is to use the nonlinear dynamic method to analyze bubble oscillation, such phenomena as bifurcation, chaos and even stimulated scattering process are investigated. The concepts of scattering and stimulated scattering are in the framework of wave process theory,[22] while the concepts of bifurcation and chaos belong to dynamic category. However, the bubble can also be regarded as a sound source when it is driven by a sound wave. Then the oscillation properties will influence sound scattering and stimulated sound scattering processes. Through studying the nonlinear dynamics characteristics of bubbles, the scattering field can be predicted.

In this paper, we consider the nonlinear dynamics and stimulated scattering process of an acoustically excited spherical gas bubble in water. The model used to describe the motion of the bubble radius is the Keller–Miksis equation. The complex dynamics in this bubble oscillation system can be analyzed by theoretical and numerical analysis. The threshold value of chaotic motion are obtained by using Lyapunov exponent and Melnikov's method, and numerical simulations not only show the consistence with the theoretical analysis but also exhibit the bifurcation diagrams and frequency response diagrams with more complex dynamical behaviors, including bifurcation, chaos and even stimulated scattering process.

The rest of the paper is organized as follows. The model of a single bubble oscillation is described in Section 2. The theoretical analysis of bubble dynamics, including the calculation formula of Lyapunov exponent and the threshold analysis used by Melnikov's method is derived in Section 3. In Section 4 presented are the numerical simulation results which give support to the theoretical analysis and also reveal more important phenomena in a bubble oscillation system. Finally, some conclusions drawn from the present study are in Section 5.

2. Model of a single bubble oscillation

In order to model large amplitude oscillations of a single gas bubble in water, the compressibility of the liquid must be taken into account. The Keller–Miksis equation is a most accurate one,[1] which can be used to describe the evolution of radius of the acoustically excited spherical gas bubble with time

$$\begin{aligned}\left(1-\frac{\dot{R}}{c}\right)R\ddot{R}+\frac{3}{2}\left(1-\frac{\dot{R}}{3c}\right)\dot{R}^2 &= \left(1+\frac{\dot{R}}{c}\right)\frac{p_1}{\rho}+\frac{R}{\rho c}\frac{\mathrm{d}p_1}{\mathrm{d}t}, \quad (1)\\ p_1 &= \left(P_{\mathrm{stat}}+\frac{2\sigma}{R_{\mathrm{n}}}-P_{\mathrm{V}}\right)\left(\frac{R_{\mathrm{n}}}{R}\right)^{3\kappa}-P_{\mathrm{stat}}\\ &\quad +P_{\mathrm{V}}-\frac{2\sigma}{R}-\frac{4\eta}{R}\dot{R}+p(t), \quad (2)\\ p(t) &= -P_{\mathrm{a}}\sin(2\pi v_{\mathrm{a}}t), \quad (3)\end{aligned}$$

where R is the spherical bubble radius, whose variation with time t, $R(t)$, needs to be determined; $\dot{R}$ is the change rate of the bubble radius; $\ddot{R}$ is the change rate of impulse speed; R_{n} is the radius of the bubble at rest, and covers the range from below a micrometer to several millimeters; κ is the polytropic exponent of the gas in the bubble; ρ, η, σ, and c are the density, the viscosity, the surface tension of the liquid, and the sound speed in the liquid, respectively; P_{stat} is the static pressure of the environment; P_{V} is the vapor pressure inside the bubble; $p(t)$ is the external pressure imposed on the bubble wall. In the case of a single frequency sound excitation of the bubble, it can be written in the form varying sinusoidally with frequency v_{a} and having a pressure amplitude P_{a}. The driving frequency v_{a} typically takes values from a few hertz to a few megahertz, and the driving pressure amplitude P_{a} may reach several megapascal.[10]

The Keller–Miksis equation can be reformulated as a set of autonomous differential equations of first order:

$$\begin{aligned}\dot{R} &= U, \quad (4)\\ \dot{U} &= \left[-\frac{U^2}{2}\left(3-\frac{U}{c}\right)+\left(1+(1-3\kappa)\frac{U}{c}\right)\right.\\ &\quad \times\left(\frac{P_{\mathrm{stat}}-P_{\mathrm{V}}}{\rho}+\frac{2\sigma}{\rho R_{\mathrm{n}}}\right)\left(\frac{R_{\mathrm{n}}}{R}\right)^{3\kappa}\\ &\quad -\frac{4\mu}{\rho}\frac{U}{R}-\left(1+\frac{U}{c}\right)\frac{P_{\mathrm{stat}}-P_{\mathrm{V}}+P_{\mathrm{a}}\sin(2\pi\theta)}{\rho}\\ &\quad \left.-\frac{2\sigma}{\rho R}-R\frac{2\pi v_{\mathrm{a}}P_{\mathrm{a}}}{\rho c}\cos(2\pi\theta)\right]\Big/\left[\left(1-\frac{U}{c}\right)R+\frac{4\eta}{\rho c}\right], \quad (5)\\ \dot{\theta} &= v_{\mathrm{a}}, \quad (6)\end{aligned}$$

where the third variable θ is introduced for eliminating variable t. The complex dynamics in this bubble oscillation system can be analyzed by theoretical and numerical analysis in the next section.

3. Theoretical analysis of bubble dynamics

3.1. Lyapunov exponent analysis

Lyapunov exponent (LE) is an important quantity of nonlinear dynamics analysis, and the LE of the dynamical system is a quantity that characterizes the separation rate of infinitesimally close trajectories. It plays a crucial role in identifying the dynamic behavior and chaotic degree of strange attractor. In this paper, the Jacobian matrix algorithm is used to calculate the Lyapunov exponent of the chaotic system. The autonomous equations (4)–(6) are shown as follows.

$$\begin{cases} \dot{R} = f_1(R,U,\theta) = U, \\ \dot{U} = f_2(R,U,\theta) = u/v, \\ \dot{\theta} = f_3(R,U,\theta) = v_{\rm a}, \end{cases} \tag{7}$$

$$\begin{aligned} u = & -\frac{U^2}{2}\left(3-\frac{U}{c}\right)+\left(1+(1-3\kappa)\frac{U}{c}\right) \\ & \times\left(\frac{P_{\rm stat}-P_{\rm V}}{\rho}+\frac{2\sigma}{\rho R_{\rm n}}\right)\left(\frac{R_{\rm n}}{R}\right)^{3\kappa} \\ & -\frac{4\mu}{\rho}\frac{U}{R}-\left(1+\frac{U}{c}\right)\frac{P_{\rm stat}-P_{\rm V}+P_{\rm a}\sin(2\pi\theta)}{\rho} \\ & -\frac{2\sigma}{\rho R}-R\frac{2\pi v_{\rm a}P_{\rm a}}{\rho c}\cos(2\pi\theta), \end{aligned} \tag{8}$$

$$v = \left(1-\frac{U}{c}\right)R+\frac{4\mu}{\rho c}. \tag{9}$$

The form of the Jacobian matrix is

$$\begin{aligned} \boldsymbol{J} &= \begin{bmatrix} \frac{{\rm d}f_1}{{\rm d}R} & \frac{{\rm d}f_1}{{\rm d}U} & \frac{{\rm d}f_1}{{\rm d}\theta} \\ \frac{{\rm d}f_2}{{\rm d}R} & \frac{{\rm d}f_2}{{\rm d}U} & \frac{{\rm d}f_2}{{\rm d}\theta} \\ \frac{{\rm d}f_3}{{\rm d}R} & \frac{{\rm d}f_3}{{\rm d}U} & \frac{{\rm d}f_3}{{\rm d}\theta} \end{bmatrix} \\ &= \begin{bmatrix} 0 & 1 & 0 \\ \frac{u'_R v - u v'_R}{v^2} & \frac{u'_U v - u v'_U}{v^2} & \frac{u'_\theta v - u v'_\theta}{v^2} \\ 0 & 0 & 0 \end{bmatrix}, \end{aligned} \tag{10}$$

where

$$\begin{aligned} u'_R = & -\frac{3\kappa}{R}\left(1+(1-3\kappa)\frac{U}{c}\right)\left(\frac{P_{\rm stat}-P_{\rm V}}{\rho}+\frac{2\sigma}{\rho R_{\rm n}}\right)\left(\frac{R_{\rm n}}{R}\right)^{3\kappa} \\ & +\frac{2\sigma}{\rho R^2}+\frac{4\mu U}{\rho R^2}-\frac{2\pi v_{\rm a}P_{\rm a}}{\rho c}\cos(2\pi\theta), \end{aligned} \tag{11}$$

$$v'_R = 1-\frac{U}{c}, \tag{12}$$

$$\begin{aligned} u'_U = & -3U+\frac{3U^2}{2c}+\frac{(1-3\kappa)}{c}\left(\frac{P_{\rm stat}-P_{\rm V}}{\rho}+\frac{2\sigma}{\rho R_{\rm n}}\right)\left(\frac{R_{\rm n}}{R}\right)^{3\kappa} \\ & -\frac{4\mu}{\rho R}-\frac{P_{\rm stat}-P_{\rm V}+P_{\rm a}\sin(2\pi\theta)}{\rho c}, \end{aligned} \tag{13}$$

$$v'_U = -\frac{R}{c}, \tag{14}$$

$$\begin{aligned} u'_\theta = & -\left(1+\frac{U}{c}\right)\frac{2\pi P_{\rm a}\cos(2\pi\theta)}{\rho} \\ & +R\frac{(2\pi)^2 v_{\rm a}P_{\rm a}\sin(2\pi\theta)}{\rho c}, \end{aligned} \tag{15}$$

$$v'_\theta = 0. \tag{16}$$

A system may have more than one LE. In this bubble oscillation system, there are three LEs. Then, to detect the onset of chaos, only the largest Lyapunov exponent $\lambda_{\rm max}$ needs to be calculated. The intermediate situation of $\lambda_{\rm max}$=0 signifies a neutrally stable orbit. If $\lambda_{\rm max}$<0, the disturbed trajectory is attracted eventually to a stable periodic. By contrast, $\lambda_{\rm max}$>0 denotes an unstable and chaotic trajectory.

3.2. Melnikov analysis

The threshold value of chaotic motion under the periodic perturbation is obtained by using Melnikov's method. By utilizing the relationship between bubble volume V and bubble radius R, $V=\frac{4}{3}\pi R^3$, the equation of bubble volume vibration can be described as[22]

$$\ddot{V}+\omega_0^2 V-\alpha V^2-\beta\left(2\ddot{V}\dot{V}+\dot{V}^2\right)+\upsilon_1 V^3+\delta\dot{V}=\chi p, \tag{17}$$

where $\alpha=\omega_0^2(\kappa+1)/2V_0$, $\upsilon_1=(\kappa+1)(\kappa+2)\omega_0^2/6V_0^2$, $\beta=(8\pi R_0^3)^{-1}$, $V_0=\frac{4}{3}\pi R_0^3$ is the equilibrium volume of a single bubble, $\delta=R_0/c_0\omega_0^2$ is the dissipative coefficient, $\chi=4\pi R_0/\rho_0$ is the external excitation coefficient, and ω_0 is the resonance frequency of bubble oscillation.

When the frequency of the acoustic pressure is close to the natural frequency of the bubble oscillation, equation (17) can be simplified into

$$\ddot{V}+\delta\dot{V}+\omega_0^2 V+\left(3\beta\omega_0^2-\alpha\right)V^2+\upsilon_1 V^3=\chi p. \tag{18}$$

Let $X=V$, its canonical form is

$$\begin{cases} \dot{X}=Y, \\ \dot{Y}=-\omega_0^2 X-(3\beta\omega_0^2-\alpha)X^2-\upsilon_1 X^3-\delta Y+\chi p, \end{cases} \tag{19}$$

When neither external excitation nor dissipation effect exists, i.e., $\delta=\chi=0$, the bubble oscillation system is a conserved, Hamiltonian system with Hamiltonian function

$$H(X,\dot{X})=\frac{1}{2}\dot{X}+\frac{\omega_0^2}{2}X^2+\frac{3\beta\omega_0^2-\alpha}{3}X^3+\frac{\upsilon_1}{4}X^4. \tag{20}$$

In this system, there are three singularities:

$$P_0=(0,0),\ P_1=(a,0),\ P_2=(b,0), \tag{21}$$

where

$$a=\frac{(3\beta\omega_0^2-\alpha)+\sqrt{(3\beta\omega_0^2-\alpha)^2-4\omega_0^2\upsilon_1}}{2\upsilon_1},$$

and

$$b=\frac{(3\beta\omega_0^2-\alpha)-\sqrt{(3\beta\omega_0^2-\alpha)^2-4\omega_0^2\upsilon_1}}{2\upsilon_1}.$$

Then the Melnikov's method can be used to obtain the conditions for the existence of chaotic motion:

1) When $\upsilon_1>0$, $(3\beta\omega_0^2-\alpha)^2-4\omega_0^2\upsilon_1>0$ and $b<a<0$, P_1 is a saddle point, P_0 and P_2 are central points. P_1 is on the homoclinic orbit, whose parameter equations are

$$\begin{cases} X_\pm^0=\pm\dfrac{2\sqrt{2}(3\beta\omega_0^2-\alpha)}{3\upsilon_1} \\ \quad\times\dfrac{\exp\left[\pm\dfrac{3\beta\omega_0^2-\alpha}{3\sqrt{\upsilon_1}}t\right]}{\exp\left[\pm\dfrac{2(3\beta\omega_0^2-\alpha)}{3\sqrt{\upsilon_1}}t\right]+1}-\dfrac{3\beta\omega_0^2-\alpha}{3\sqrt{\upsilon_1}}, \\ Y_\pm^0=\pm\dfrac{2\sqrt{2}(3\beta\omega_0^2-\alpha)^2}{9\upsilon_1^{3/2}} \\ \quad\times\dfrac{1-\exp\left[\pm\dfrac{2(3\beta\omega_0^2-\alpha)}{3\sqrt{\upsilon_1}}t\right]}{\exp\left[\pm\dfrac{2(3\beta\omega_0^2-\alpha)}{3\sqrt{\upsilon_1}}t\right]+1}\exp\left[\pm\dfrac{3\beta\omega_0^2-\alpha}{3\sqrt{\upsilon_1}}t\right]. \end{cases} \tag{22}$$

The Melnikov function of stable or unstable manifold is

$$\begin{aligned} M(\xi_0) &= \int_{-\infty}^{+\infty}[\delta Y_\pm^0(t)+P_\mathrm{a}\cos[\omega(t+t_0)]]Y_\pm^0(t)\,\mathrm{d}t \\ &= -I_0\delta\pm I_1P_\mathrm{a}\sin(\omega t_0), \end{aligned} \tag{23}$$

where $I_0=\sqrt{2}\omega_0^2/9\upsilon_1^{3/2}$ and

$$I_1=\frac{2\sqrt{2}\pi\omega}{\upsilon_1^{1/2}}\frac{\exp\left[\dfrac{6\pi\omega\sqrt{\upsilon_1}}{|3\beta\omega_0^2-\alpha|}\right]}{1+\exp\left[\dfrac{6\pi\omega\sqrt{\upsilon_1}}{|3\beta\omega_0^2-\alpha|}\right]}.$$

2) When $\upsilon_1<0$, the equation of the heteroclinic orbit is

$$\begin{cases} X_\pm^0=\pm\dfrac{2(3\beta\omega_0^2-\alpha)}{3\upsilon_1}\dfrac{\exp\left[\pm\dfrac{\sqrt{2}(3\beta\omega_0^2-\alpha)}{3\sqrt{-\upsilon_1}}t\right]}{\exp\left[\pm\dfrac{\sqrt{2}(3\beta\omega_0^2-\alpha)}{3\sqrt{-\upsilon_1}}t\right]+1}, \\ Y_\pm^0=\pm\dfrac{2\sqrt{2}(3\beta\omega_0^2-\alpha)^2}{9\upsilon_1\sqrt{-\upsilon_1}} \\ \quad\times\dfrac{\exp\left[\pm\dfrac{\sqrt{2}(3\beta\omega_0^2-\alpha)}{3\sqrt{-\upsilon_1}}t\right]}{\left(\exp\left[\pm\dfrac{\sqrt{2}(3\beta\omega_0^2-\alpha)}{2\sqrt{-\upsilon_1}}t\right]+1\right)^2}. \end{cases} \tag{24}$$

The Melnikov function of the heteroclinic orbit is

$$\begin{aligned} M(\xi_0) &= \int_{-\infty}^{+\infty}[\delta Y_\pm^0(t)+P_\mathrm{a}\cos[\omega(t+t_0)]]Y_\pm^0(t)\,\mathrm{d}t \\ &= -I_0\delta\pm I_1P_\mathrm{a}\sin(\omega t_0), \end{aligned} \tag{25}$$

where

$$I_0=\frac{2\sqrt{2}(3\beta\omega_0^2-\alpha)^3}{81\upsilon_1^2\sqrt{-\upsilon_1}},$$

and

$$I_1=\frac{2\sqrt{2}\pi\omega}{\sqrt{-\upsilon_1}}\frac{\exp\left[\dfrac{3\pi\omega\sqrt{-\upsilon_1}}{\sqrt{2}(3\beta\omega_0^2-\alpha)}\right]}{1+\exp\left[\dfrac{3\sqrt{2}\pi\omega\sqrt{-\upsilon_1}}{3\beta\omega_0^2-\alpha}\right]}.$$

So, the cross section of stable manifold and unstable manifold exists when $P_\mathrm{a}/\delta>I_0/I_1$. It is seen that the threshold value of chaotic motion should achieve a certain acoustic pressure amplitude P_a.

3.3. Stimulated scattering in a liquid with gas bubble

On the one hand, the problem of acoustic radiation from a single, slightly pulsating bubble is well understood. The effect of liquid compressibility on the motion is not important in the near field, but it will be properly considered below.[22] For an incompressible liquid, the velocity potential φ and the velocity $v=\partial\varphi/\partial r$ of the radial sound field in the liquid are described by

$$\phi(r,t)=-\dot{R}R^2/r \quad\text{and}\quad v(r,t)=\dot{R}R^2/r^2, \tag{26}$$

which provides the theoretical foundation of analyzing the radiation and scattering of sound on a bubble. The problems of radiation and scattering of sound on a single bubble are discussed in many studies.

On the other hand, let all the bubbles have an identical radius R_0 and quality factor Q near the resonant frequency ω_0, which case is similar to Raman scattering where light interacts with molecular vibration having a specified resonant frequency. The problem of stimulated scattering is reduced to the solution of the wave equation,[23]

$$\frac{\partial^2p}{\partial x^2}-\frac{1}{c_0^2}\frac{\partial^2p}{\partial t^2}=-\rho_0N\frac{\partial^2V}{\partial t^2}. \tag{27}$$

Through studying the nonlinear dynamic characteristics of a bubble, we can investigate the scattering of the external acoustic field in the next stage. The oscillatory behavior of a single bubble offers a valuable insight into the acoustic radiation and has an important foundation for understanding the principle of stimulated sound scattering. That is why it is important to understand the causes and conditions. In the following, the topics briefly mentioned before will be discussed in more depth. Emphasis is placed on numerical analysis and experimental results, where available.

4. Dynamics and stimulated sound scattering properties of bubble

This section is for the numerical simulations to support the theoretical results obtained in the previous section and to

find other complex dynamics. Equations (4)–(6) can be solved by the Runge–Kutta method easily. For the Keller–Miksis dynamical systems, chaotic bubble oscillations come into existence via repeated period doubling. When a control parameter of the system is changed, the way via repeated period doubling will be observed by numerical analysis.

4.1. Acoustic pressure amplitude bifurcation diagrams and Lyapunov exponent curves

To show the richness of the dynamical behavior of an acoustically excited bubble, several bifurcation diagrams with different parameters are made. The computation of Lyapunov exponent confirms the dynamical behaviors. For this bubble oscillation model, the main parameters of interest are the bubble radius at rest, R_n, acoustic frequency, v_a, and acoustic pressure amplitude, P_a. The other parameters are connected with the properties of the liquid outside the bubble and the gas and vapour of the liquid inside the bubble. The typical values of the parameters for a bubble in water as used in the calculations with the Keller–Miksis model, are $R|_{t=0} = R_n$, $dR/dt = 0$, $\rho = 998\ \mathrm{kg/m^3}$, $\sigma = 0.0725\ \mathrm{N/m}$, $\eta = 0.001\ \mathrm{Pa\cdot s}$, $P_{stat} = 1\times10^5\ \mathrm{Pa}$, $P_V = 2.33\ \mathrm{kPa}$, $c = 1500\ \mathrm{m/s}$, and $\kappa = 4/3$. For example, for a bubble with a radius at rest $R_n = 100\ \mu\mathrm{m}$, the linear resonance frequency f_0 described by the Keller–Miksis equation is

$$f_0 = \frac{1}{2\pi R_n\sqrt{\rho}}\sqrt{3\kappa\left(P_{stat}+\frac{2\sigma}{R_n}-P_V\right)-\frac{2\sigma}{R_n}-\frac{4\eta^2}{\rho R_n^2}} \approx 35.45\ \mathrm{kHz}. \tag{28}$$

Figure 1 gives a typical bubble oscillation example with the acoustic frequencies of $v_a = f_0$, $v_a = 0.5f_0$ and $v_a = 2f_0$ respectively. The acoustic pressure amplitude P_a in this example varies from 10kPa to 1000kPa (sound pressure level ranges from 200 dB to 240 dB).

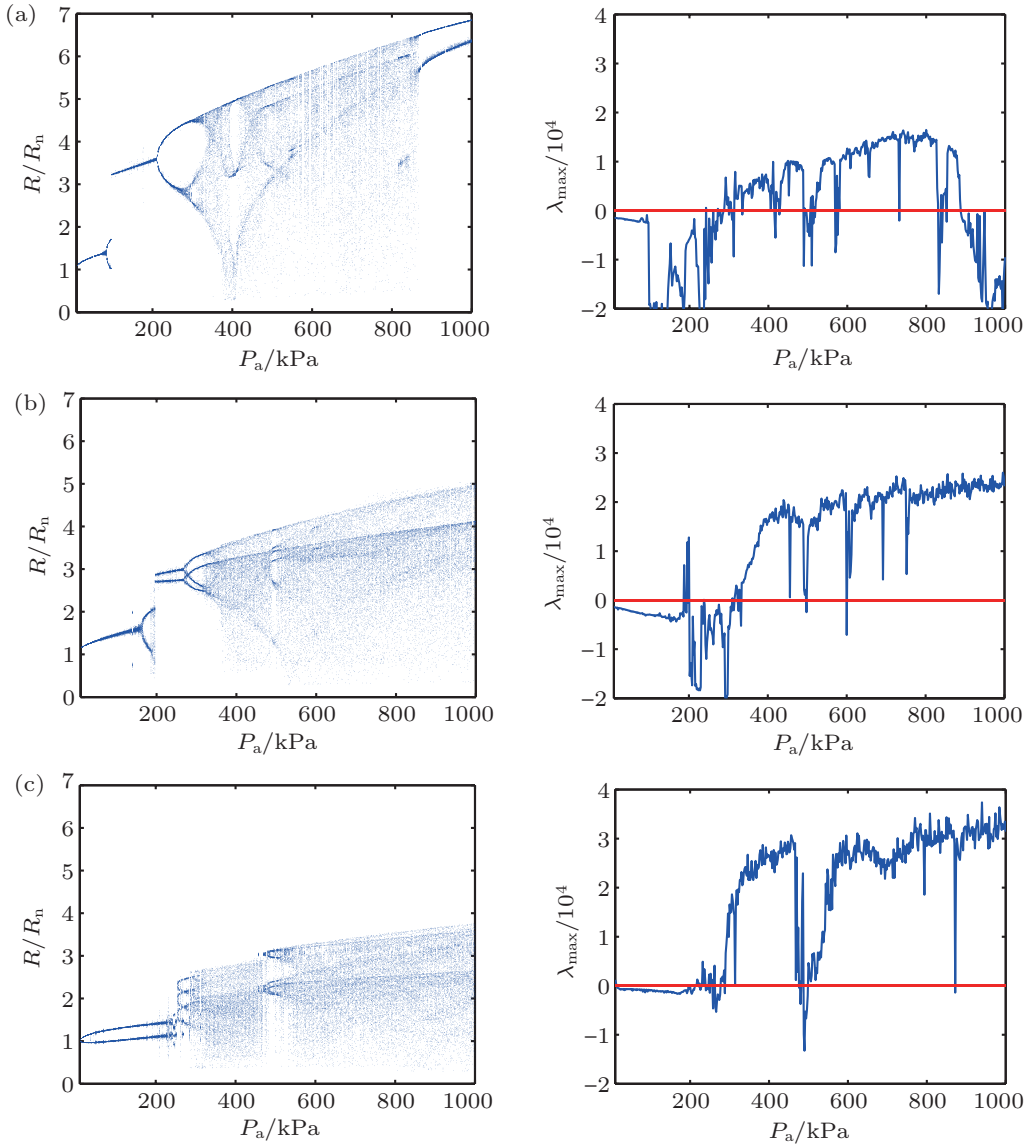


Fig. 1. (color online) Acoustic pressure amplitude bifurcation diagrams and Lyapunov exponent curves in the cases of (a) driving frequency $v_a = 0.5f_0$, (b) $v_a = f_0$, and (c) $v_a = 2f_0$.

Two different representations of the same oscillation are given in a row. There are, from left to right, acoustic pressure amplitude bifurcation diagrams, Lyapunov exponent curves. In the left row, there are the bifurcation diagrams with a fully developed period doubling cascading to chaotic oscillation for different acoustic frequencies. In the right row, there are the associated largest Lyapunov exponent $\lambda_{\max}$ curves. The maximum Lyapunov exponent $\lambda_{\max}$ is lower than zero for periodic oscillations, being zero at period doubling bifurcation points, and larger than zero for chaotic oscillation.

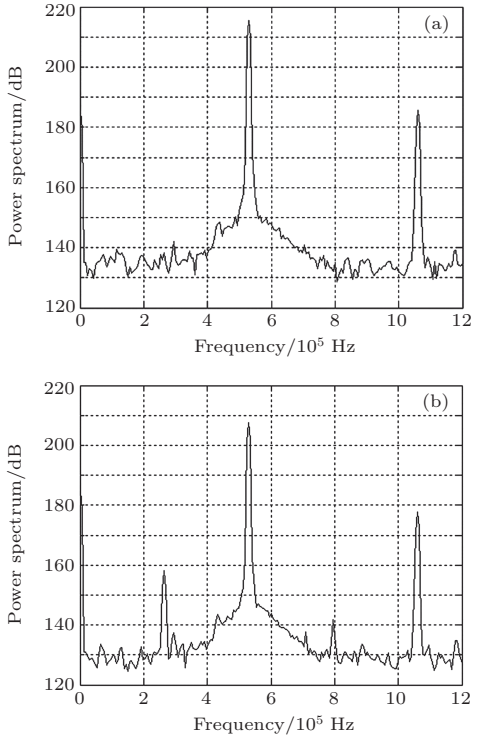


Fig. 2. Power spectrum with send-receive distance of 0.3 m (a) without and (b) with bubbles.

In the condition of typical bubble radius at rest $R_n = 100$ μm, it is shown that the dynamic characteristics of the system are more and more complex with the increasing of acoustic pressure amplitude. When acoustic pressure amplitude is above 100 kPa (220 dB), bifurcation appears, which represents that the system is in an unstable state. When acoustic pressure amplitude is between 600 kPa and 800 kPa (235.6 dB and 238.1 dB), the system is in chaotic state stably. Fixing the bubble radius at rest (resonance frequency is fixed), the acoustic pressure amplitude threshold of bifurcation is minimum when $v_a = 2f_0$ ($P_a = 20$ kPa).

An experiment is conducted in a water tank with dimensions of 1.5 m×1.2 m×1 m. The bubbles are generated by the method of water electrolysis, and its resonance frequency is about 80 kHz. When the bubble oscillations are driven by high-intensity single-frequency acoustic wave (acoustic pressure level achieves 200 dB), sub-harmonics in nonlinear system should appear. It is verified that sub-harmonics can appear when the excited acoustic pressure is not too high (as shown in Fig. 2). However, the power of generated sub-harmonic is far smaller than the power of fundamental harmonic, which implies that the system status is still in a primary stage of bifurcation.

4.2. Lyapunov exponent maps

In this section, we present a summary of single bubble dynamics by means of Lyapunov exponent maps with respect to the driving pressure and frequency. This is to outline the critical role of the control parameters in bubble dynamics and to represent an outlook of the bubble dynamics complexity. The Lyapunov exponent map of an acoustically driven bubble is depicted in Fig. 3. It is clearly seen that the two control parameters are scaled together. The threshold value of chaotic motion can be obtained in this map clearly. The parameters are shown as follows: the bubble radius at rest is $R_n = 100$ μm, the range of the studied frequency is from $0.1f_0$ to $10f_0$, and the pressure varies from 10 kPa to 1000 kPa.

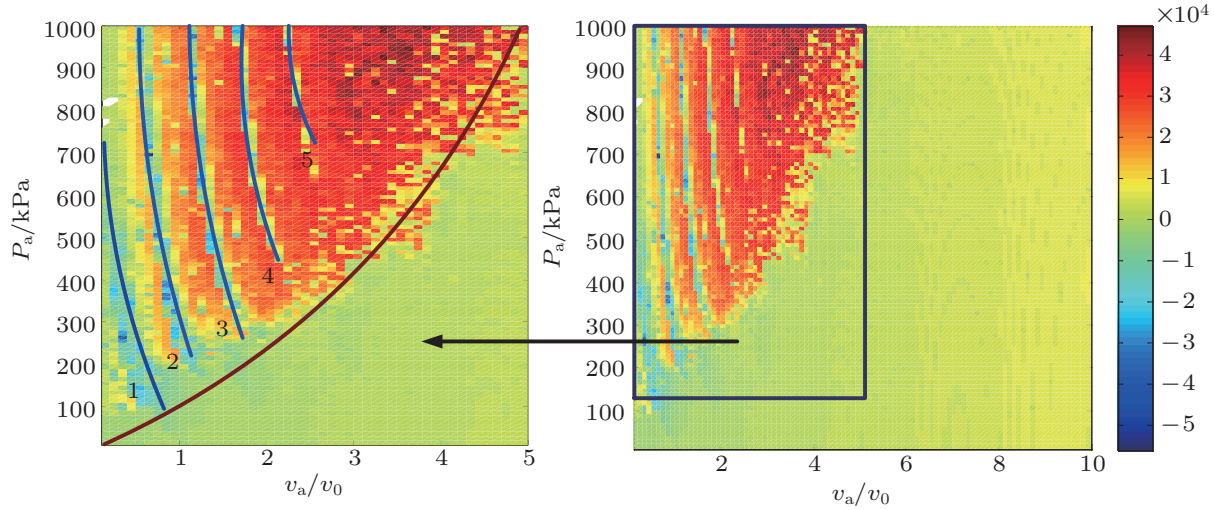


Fig. 3. (color online) Lyapunov exponent map of an acoustically driven bubble. The bubble radius at rest is $R_n = 100$ μm. The range of the studied frequency is from $0.1f_0$ to $10f_0$, and the pressure varies from 10 kPa to 1000 kPa.

The map can be divided into two parts by a red color curve in the left of the figure. It is clearly shown that it is difficult to achieve the chaotic status when the normalized frequency is higher than 5. The system becomes extremely chaotic which maintains the whole remaining pressure interval between 750 kPa and 1000 kPa, where the normalized frequency v_a/v_0 is between 2.5 to 5. In particular, there is a complex region in the left of the figure, where the the stable oscillation transforms into a chaotic one periodically. There are five gaps, which mean the stable oscillations between the regions of chaotic oscillations.

4.3. Frequency response diagrams

Oscillators are often described by frequency response curves, in which the frequency change is indicated. As is well known, the frequency response in a nonlinear system is much more complex than in a linear system. The frequency response curves for different bubble radii at rest driven by acoustic frequency $v_a = 50$ kHz, $v_a = 100$ kHz, $v_a = 200$ kHz, and $v_a = 400$ kHz are shown respectively in Figs. 4–7. The acoustic pressure amplitude P_a is in a range from 1 kPa to 2000 kPa. There are acoustic pressure amplitude bifurcation diagrams and associated frequency response diagrams in the left and right row respectively. The frequency response diagrams represent the acoustic pressure amplitude-normalized frequency plane (P_a, v/v_a), in which the color map represents the normalized amplitude (the maximum amplitude value in the diagram is normalized to 0 dB). For example, in the case of $R_n = 400$ μm, the normalized frequency of driving frequency equals 1, and the normalized frequency of linear resonance frequency of a bubble is about 0.1. In the common situation, the maximum normalized amplitude responds to the one of driving frequency, which is 0 dB.

When the linear resonance frequency of a bubble, f_0, is much smaller than the driving frequency v_a, there exists a special frequency response, including bubble linear resonance frequency f_0, excitation frequency v_a, Stokes frequency $v_a - f_0$, and anti-Stokes frequency $v_a + f_0$. This phenomenon is similar to the stimulated Raman scattering process in optics.

Frequency response diagrams can provide more details about the change of frequency component during the change of control parameter. With the increasing of acoustic pressure amplitude, more complex dynamics characteristics will arise, such as stimulated scattering, period-2, period-3, period-4, period-5, ..., chaos, etc.

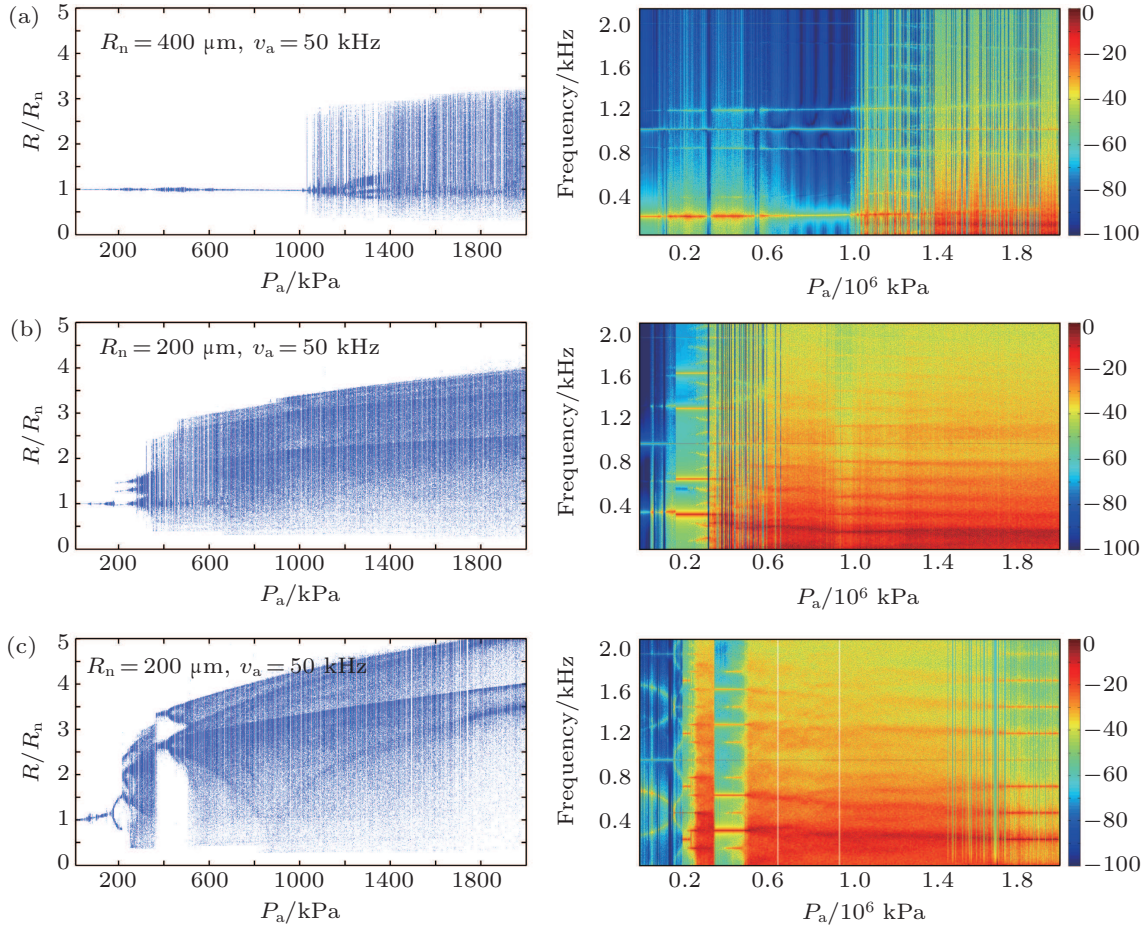


Fig. 4. (color online) Acoustic pressure amplitude bifurcation diagrams and frequency response diagrams versus acoustic pressure amplitude when driving frequency $v_a = 50$ kHz for (a) $R_n = 400$ μm ($f_0 = 8.823$ kHz, and responding normalized frequency is 0.1764), (b) $R_n = 200$ μm ($f_0 = 17.673$ kHz, and responding normalized frequency is 0.3534), and (c) $R_n = 100$ μm ($f_0 = 35.450$ kHz, and normalized to 0.7090).

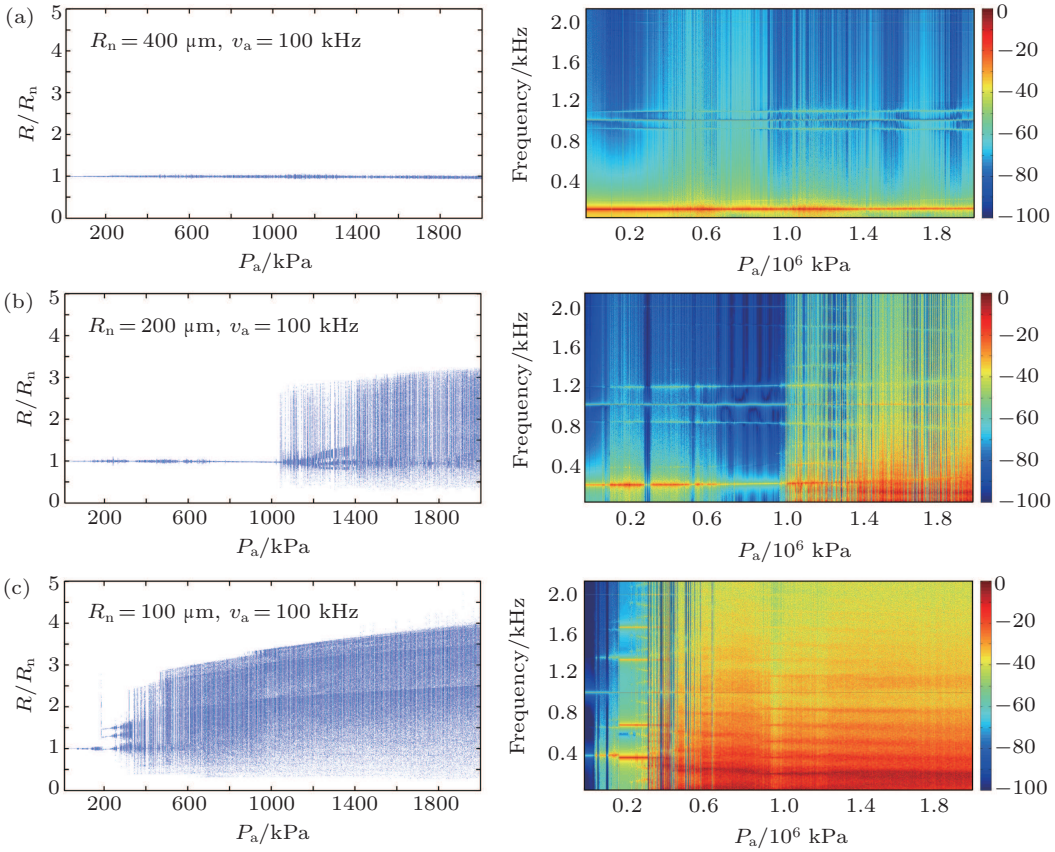


Fig. 5. (color online) Acoustic pressure amplitude bifurcation diagrams and frequency response diagrams versus acoustic pressure amplitude when driving frequency $v_a = 100$ kHz for (a) $R_n = 400$ μm ($f_0 = 8.823$kHz, and responding normalized frequency is 0.0882), (b) $R_n = 200$ μm ($f_0 = 17.673$ kHz, and responding normalized frequency is 0.1767), and (c) $R_n = 100$ μm ($f_0 = 35.450$ kHz, and normalized to 0.3545).

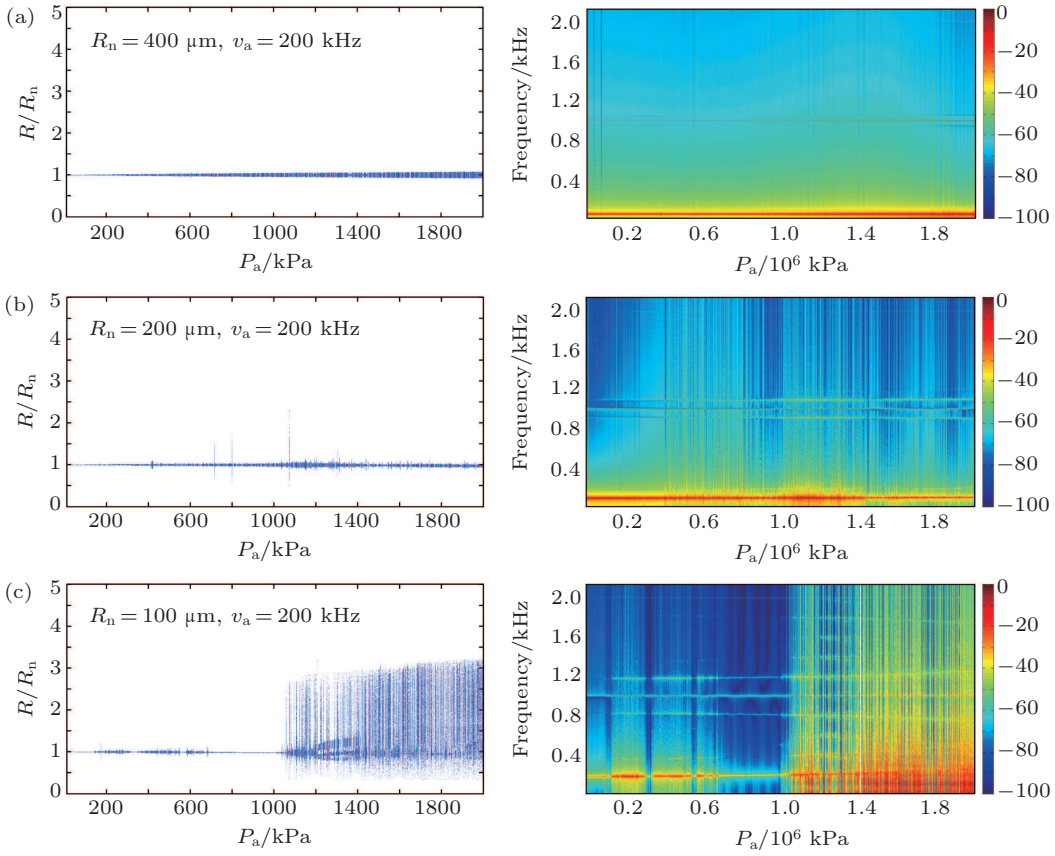


Fig. 6. (color online) Acoustic pressure amplitude bifurcation diagrams and frequency response diagrams versus acoustic pressure amplitude when driving frequency $v_a = 200$ kHz for (a) $R_n = 400$ μm ($f_0 = 8.823$ kHz, and responding normalized frequency is 0.0441), (b) $R_n = 200$ μm ($f_0 = 17.673$ kHz, and responding normalized frequency is 0.0884), and (c) $R_n = 100$ μm ($f_0 = 35.450$ kHz, and normalized to 0.1772).

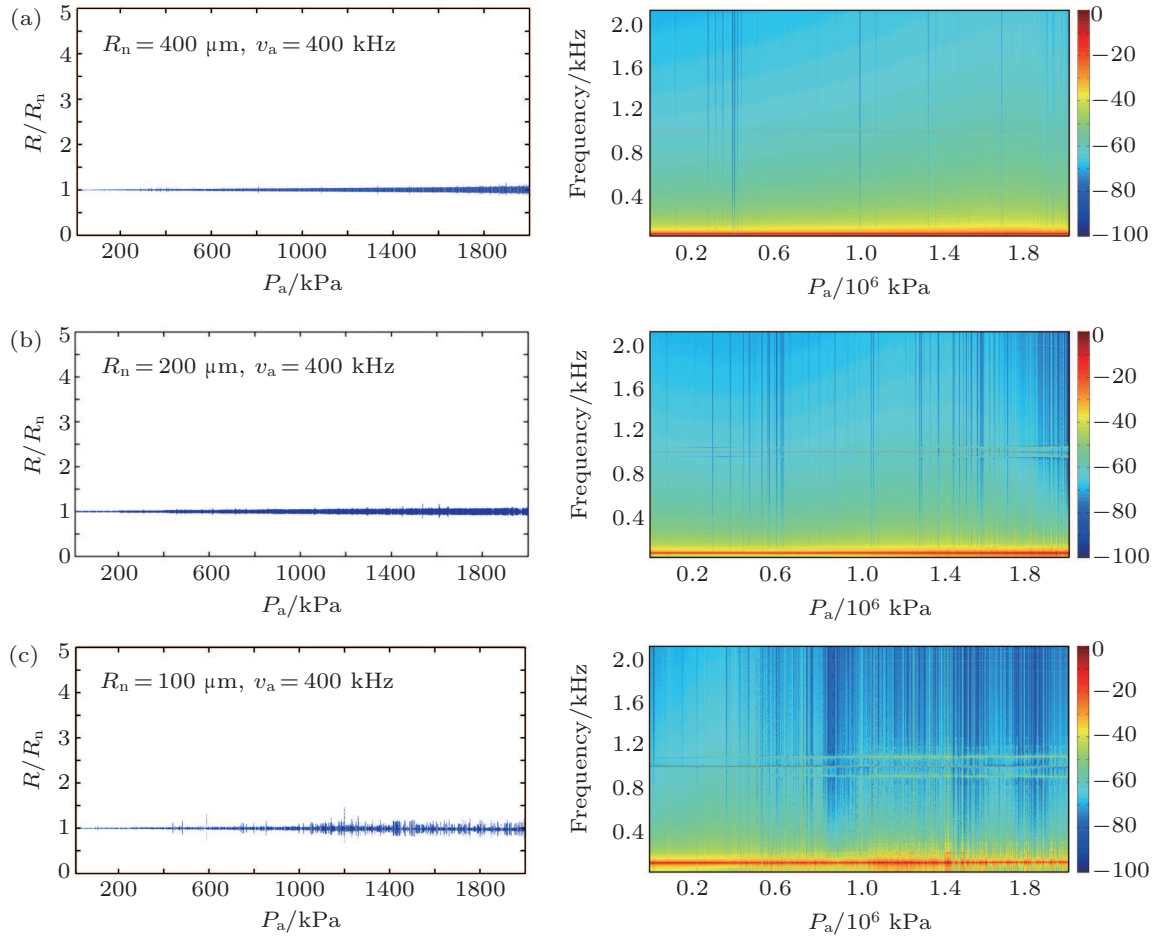


Fig. 7. (color online) Acoustic pressure amplitude bifurcation diagrams and frequency response diagrams versus acoustic pressure amplitude when driving frequency $v_a = 400$ kHz for (a) $R_n = 400$ μm ($f_0 = 8.823$ kHz, and responding normalized frequency is 0.0221), (b) $R_n = 200$ μm ($f_0 = 17.673$ kHz, and responding normalized frequency is 0.0442), and (c) $R_n = 100$ μm ($f_0 = 35.450$ kHz, and normalized to 0.0886).

It is shown that the stimulated sound scattering process happens much more easily when the linear resonance frequency of a bubble f_0 is much smaller than the driving frequency v_a. There exist two additional frequency components increasing or decreasing near the driving frequency v_a stably. These are special phenomena in the process of stimulated sound scattering on a bubble due to the nonlinear interaction between linear resonance frequency and driving frequency. The two frequency components are Stokes component (its frequency $f_- = v_a - f_0$) and anti-Stokes component (its frequency $f_+ = v_a + f_0$), respectively.

With the increasing of the linear resonance frequency of a bubble f_0, it is much more difficult for the stimulated sound scattering to occur. The bifurcation and chaos may play an important role in the bubble oscillation.

4.4. Threshold of stimulated sound scattering

Examples of the phenomenon of stimulated sound scattering are given above. The threshold of stimulated sound scattering is associated with three major parameters, i.e., the bubble radius at rest (linear resonance frequency of bubble), acoustic frequency, and acoustic pressure amplitude. The threshold is much smaller when the ratio f_0/v_a is not close to 1, meanwhile the P_a is not too big. On the one hand, when the f_0 is close to v_a, the bifurcation may arise easily. On the other hand, with the increasing of P_a, the nonlinear resonance of a bubble may be destroyed by the state of chaos.

It is shown that the threshold of stimulated sound scattering is smaller than the ones of bifurcation and chaos in the common condition. When the bubble radius at rest decreases from $R_n = 400$ μm to $R_n = 100$ μm, the phenomenon of stimulated sound scattering gradually disappears as acoustic pressure amplitude increases. The interesting phenomenon shows that the bigger the bubble radius at rest, the larger the range of stimulated sound scattering is. For example, the phenomenon stimulated sound scattering will exist until $P_a = 2000$ kPa for $R_n = 400$ μm, but the phenomenon can only exist till $R_n = 100$ μm. On the other hand, it is easy to find out that the smaller the bubble radius at rest, the lower the acoustic pressure amplitude threshold from the bifurcation diagrams is. The system is not chaotic even when the driving amplitude achieves $P_a = 200$ kPa when the bubble radius at rest

$R_n = 400$ μm. The threshold of chaos for $R_n = 200$ μm is about 100 kPa. However, in the condition of $R_n = 100$ μm, the system gradually comes into bifurcation only at $P_a = 20$ kPa.

Stimulated sound scattering is a special phenomenon which is associated with bubble nonlinear oscillation. Stimulated sound scattering is different from bifurcation and chaos, which is the result of the nonlinear resonance of a bubble under the excitation of high-amplitude acoustic sound wave essentially.

4.5. Frequency response curve

There is no doubt that the frequency responses of the system are complex versus acoustic pressure amplitude. The further research will focus on the variation of driving frequency, then we can obtain more detailed information about the evolution of this bubble oscillation system.

From the acoustic pressure amplitude-normalized frequency plane in frequency response diagrams, it is obvious that the frequency response of the system relies on the acoustic pressure amplitude. The power spectrum is a common method to characterize a nonlinear oscillation by its spectral content. Figure 8 gives a set of power spectrum diagrams of the oscillation system response versus acoustic pressure amplitude. There simulation results have taken the bubble radius at rest $R_n = 200$ μm ($f_0 = 17.73$ kHz) and acoustic frequency$v_a = 100$ kHz as example.

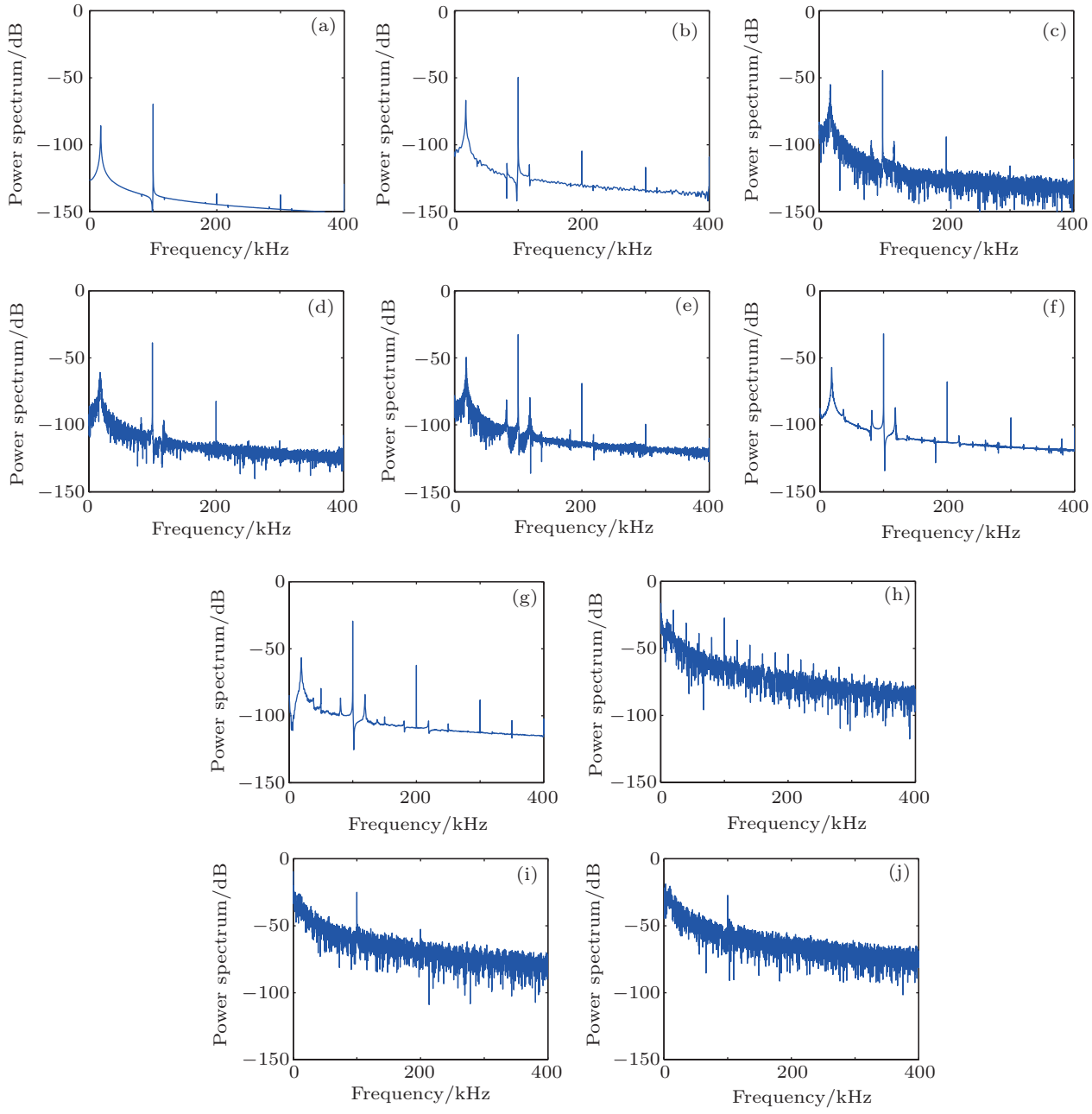


Fig. 8. (color online) Power spectrum diagrams of the oscillation system response versus acoustic pressure amplitude at (a) $P_a = 10$ kPa (200 dB), (b) $P_a = 100$ kPa (220 dB), (c) $P_a = 180$ kPa (225 dB), (d) $P_a = 350$ kPa (230 dB), (e) $P_a = 700$ kPa (237 dB), (f) $P_a = 750$ kPa (237.5 dB), (g) $P_a = 1000$ kPa (240 dB), (k) $P_a = 1400$ kPa (242 dB), (i) $P_a = 2000$ kPa (246 dB), and (j) $P_a = 2500$ kPa (248 dB).

When the acoustic pressure amplitude $P_a = 200$ dB, besides the driving frequency and its harmonics, there is only linear frequency response component in the system. When the driving amplitude reaches 220 dB, the special components, i.e., Stokes component and the anti-Stokes component arise, and the amplitudes of all the components increase as acoustic pressure amplitude increases. In the case of driving amplitude $P_a = 237$ dB, the system comes into period 5. Subharmonic components arise till $P_a = 240$ dB in the system, which shows that the system comes into bifurcation. With further increasing P_a, the frequency response of the system becomes more and more complex. When the amplitude achieves 248dB, the system is already chaotic. It looks like a noise spectrum. With the same excitation frequency, the oscillation can reach different states, such as stimulated scattering, period-2, period-4, period-5, ..., chaos, etc.

5. Conclusions

In this article, the nonlinear dynamics of an acoustically excited gas bubble in water is investigated by theoretical and numerical analysis methods. The evolution of the bubble radius with time is modeled by using the Keller–Miksis equation, which takes into account the compressibility of the liquid. Our results show the bubble radius has strongly nonlinear behavior with respect to the pressure amplitude and excitation frequency as the control parameters, and give an intuitive insight into stimulated sound scattering on a bubble.

On the one hand, the Jacobian matrix is derived for calculating Lyapunov exponent, and the threshold values of chaotic motion under the periodic perturbation are obtained by using Melnikov's method. The numerical simulations not only show the consistence with the theoretical analysis but also exhibit the bifurcation diagrams and Lyapunov exponent maps, which help to determine the chaotic states under many control parameters.

On the other hand, stimulated sound scattering is a special phenomenon which is associated with bubble nonlinear oscillation. Based on the Keller–Miksis equation, the phenomenon and threshold of stimulated sound scattering can be obtained by using a numerical analysis method and frequency response diagrams. The stimulated sound scattering is different from common dynamical behaviors, such as bifurcation and chaos, which is the consequence of the nonlinear resonance of a bubble under the excitation of high-amplitude acoustic sound wave essentially. The numerical analysis results show that the threshold of stimulated sound scattering is smaller than the ones of bifurcation and chaos in the common condition.

References

[1] Keller J B and Miksis M 1980 *J. Acoust. Soc. Am.* **68** 628
[2] Brennen C E 1995 *Cavitation and Bubble Dynamics* (New York: Oxford University Press) pp. 123–125
[3] Leighton T G 1994 *The Acoustic Bubble* (London: Academic Press) pp. 356–370
[4] Wang C H and Cheng J C 2014 *Acta Phys. Sin.* **63** 134301 (in Chinese)
[5] Chen W Z, Liu Y N, Huang W and Gao X X 2006 *Sci. China-Phys. Mech. Astron.* **49** 385
[6] Li B B, Zhang H C, Han B and Lu J 2012 *Sci. China-Phys. Mech. Astron.* **55** 1291
[7] Yang D S, Shi J, Shi S G, Zhang H Y, Jiang W and Jin S Y 2013 *Acta Acustica* **32** 115 (in Chinese)
[8] Zhu Z M and Du G H 1995 *Acta Acustica* **20** 425 (in Chinese)
[9] Eller A and Flynn H G 1969 *J. Acoust. Soc. Am.* **46** 722
[10] Lauterborn W and Kurz T 2010 *Rep. Prog. Phys.* **73** 106501
[11] Miksis M J and Ting L 1989 *J. Acoust. Soc. Am.* **86** 2349
[12] Chen Q, Zou X Y and Cheng J C 2006 *Acta Phys. Sin.* **55** 6476 (in Chinese)
[13] Shen Z Z and Lin S Y 2011 *Acta Phys. Sin.* **60** 104302 (in Chinese)
[14] Wang C H and Lin S Y 2010 *Chin. J. Theor. Appl. Mech.* **42** 1050
[15] Lauterborn W, Kurz T, Mettin R, Koch P, Kroninger D and Schanz D 2008 *Arch. Acoust.* **33** 609
[16] Behnia S, Jafari A, Soltanpoor W and Jahanbakhsh O 2009 *Chaos, Solitons and Fractals* **41** 818
[17] Ren S, Zhang J Z and Li K L 2012 *Chin. Phys. Lett.* **29** 020504
[18] Bunkin F V, Vlasov D V and Zabolotskaya E A 1983 *Akust. Zh.* **29** 169 (in Russian)
[19] Zabolotskaya E A and Kravtsov Y A 1985 *Akust. Zh.* **31** 338 (in Russian)
[20] Zabolotskaya E A 1984 *Akust. Zh.* **30** 324 (in Russian)
[21] Butkovskii O Y, Zabolotskaya E A and Kravtsov Y A 1987 *Akust. Zh.* **33** 163 (in Russian)
[22] Naugolnykh K A and Ostrovsky L A 1998 *Nonlinear Wave Processes in Acoustics* (New York: Cambridge University Press) pp. 16–20, 261–265
[23] Ilinskii Y A and Zabolotskaya E A 1992 *J. Acoust. Soc. Am.* **92** 2837